

NACA RM L56H13

UNCLASSIFIED

C.1

~~CONFIDENTIAL~~
NACA

RESEARCH MEMORANDUM

STATIC STABILITY CHARACTERISTICS OF A CAMBERED-DELTA-WING
MODEL AT HIGH SUBSONIC SPEEDS

By William C. Moseley, Jr. ✓

Langley Aeronautical Laboratory
Langley Field, Va.

CLASSIFICATION CHANGED

UNCLASSIFIED

LIBRARY COPY

NOV 2 1956

By authority of *Nasa PA-1*
Officer Date *9/17/58*
CLASSIFIED DOCUMENT *95A*

LANGLEY AERONAUTICAL LABORATORY
LIBRARY NACA
LANGLEY FIELD, VIRGINIA

This material contains information affecting the National Defense of the United States within the meaning of the espionage laws, Title 18, U.S.C., Secs. 793 and 794, the transmission or revelation of which in any manner to an unauthorized person is prohibited by law.

NATIONAL ADVISORY COMMITTEE FOR AERONAUTICS

WASHINGTON

October 31, 1956

~~CONFIDENTIAL~~

UNCLASSIFIED

NATIONAL ADVISORY COMMITTEE FOR AERONAUTICS

RESEARCH MEMORANDUM

STATIC STABILITY CHARACTERISTICS OF A CAMBERED-DELTA-WING
MODEL AT HIGH SUBSONIC SPEEDS

By William C. Moseley, Jr.

SUMMARY

An investigation at high subsonic speeds was made in the Langley high-speed 7- by 10-foot tunnel to determine the static stability characteristics of a cambered-delta-wing model with wing dihedral angles of 20° and 50° . The cambered delta wing was selected so that the projected plan form with a wing dihedral angle of 0° was the same as that of a 60° delta wing.

The 20° wing-dihedral configuration with tail off was generally longitudinally stable throughout the angle-of-attack range tested for all Mach numbers. The 50° wing-dihedral configuration was generally longitudinally stable except for a range of neutral stability near an angle of attack of 17° at a Mach number of 0.80 and possibly above this Mach number.

The 20° wing-dihedral configuration with tail off was directionally unstable throughout the angle-of-attack range for all Mach numbers. The 50° wing-dihedral configuration with tail off was directionally unstable at low angles of attack but became directionally stable at high angles of attack.

The tail-off effective dihedral was negative for the 20° wing-dihedral configuration at low angle of attack but increased with angle of attack until the configuration had positive effective dihedral above about an angle of attack of 5° . Increasing the wing dihedral from 20° to 50° increased the positive effective dihedral so that the configuration had positive effective dihedral throughout the angle-of-attack range.

Addition of the half-delta vertical tail to either configuration resulted in a stable increment of directional stability at low angle of attack but a loss in tail effectiveness with increasing angle of attack resulted in directional instability for some configurations in the high angle-of-attack range. The 20° wing-dihedral configuration with 30°

V-tail plus ventral fin resulted in a directionally stable configuration throughout the angle-of-attack and Mach number ranges tested. The 45° V-tail with the 50° wing-dihedral configuration was directionally stable for all angles of attack and Mach numbers investigated. However, large reductions in positive effective dihedral occurred for the 50° wing-dihedral configurations at the higher angles of attack.

INTRODUCTION

Both experiment and theory have shown that some structural and aerodynamic advantages can be obtained through the use of delta wings on aircraft. However, delta-wing configurations have shown tendencies toward loss of directional stability and effective dihedral at high angles of attack. Previous tests have indicated these tendencies can be alleviated through the use of wing dihedral (ref. 1) or wing camber (ref. 2). Low-speed tests are reported in reference 3 of a wing having both dihedral and camber for which stable configurations were obtained at high angles of attack through proper selection of wing dihedral and tail configuration. The present investigation was made to obtain data at high subsonic speeds on some of the more promising configurations of reference 3.

The wing of the present investigation is a portion of a right circular cone wherein the selection of the altitude and radius of the base dictates the amount of camber for a given plan form. The wing was formed of sheet steel and the simplicity of construction dictates its possible use on missile configurations. The projected plan form of the wing at a dihedral angle of 0° was the same as that of a 60° delta wing.

Tests were made with wing dihedral angles of 20° and 50° through an angle-of-attack range at Mach numbers from 0.60 to 0.92. Reynolds number based on the mean aerodynamic chord varied from 4.5×10^6 to 5.0×10^6 .

SYMBOLS

The data of this investigation are presented about the standard body axes as shown in figure 1. The moment coefficients are referenced about the quarter-chord point of the mean aerodynamic chord and to the fuselage center line. Coefficients and symbols are defined as follows:

C_N normal-force coefficient, $\frac{\text{Normal force}}{qS}$

~~CONFIDENTIAL~~

| | |
|------------|---|
| C_A | axial-force coefficient, $\frac{\text{Axial force}}{qS}$ |
| C_Y | side-force coefficient, $\frac{\text{Side force}}{qS}$ |
| C_m | pitching-moment coefficient, $\frac{\text{Pitching moment}}{qSt}$ |
| C_n | yawing-moment coefficient, $\frac{\text{Yawing moment}}{qSb}$ |
| C_l | rolling-moment coefficient, $\frac{\text{Rolling moment}}{qSb}$ |
| q | free-stream dynamic pressure, $\frac{\rho V^2}{2}$, lb/sq ft |
| ρ | mass density of air, slugs/cu ft |
| V | free-stream velocity, ft/sec |
| S | wing area (projected area when dihedral is 0° includes area inside of fuselage), sq ft |
| \bar{c} | mean aerodynamic chord, ft |
| b | wing span (when dihedral is 0°), ft |
| M | Mach number |
| α | angle of attack, deg |
| β | angle of sideslip, deg |
| Γ_w | wing dihedral angle (measured in plane tangent to wing surface at wing root; see fig. 2), deg |

$$C_{l\beta} = \frac{\partial C_l}{\partial \beta}$$

$$C_{n\beta} = \frac{\partial C_n}{\partial \beta}$$

$$C_{Y\beta} = \frac{\partial C_Y}{\partial \beta}$$

MODEL AND APPARATUS

Details of the test model are given in figure 2. Photographs of the model mounted on the sting in the Langley high-speed 7- by 10-foot tunnel are shown as figure 3. The 1/4-inch-sheet-steel wings were formed into the desired shape, which was obtained by using a segment of a right circular cone. The leading edge was an element of the cone with the junction of the wing leading edge and fuselage being the apex. For this investigation the cone altitude and radius of the base shown in figure 4 dictate the amount of camber for a given plan form. The wing geometry was chosen so that the projected plan form when the dihedral angle was 0° was that of a 60° delta wing. The wing leading and trailing edges were beveled to sharp edges.

For these tests wing dihedral angles of 20° and 50° were investigated since these dihedral angles give the most promising results (ref. 3). The wing was tested with a circular fuselage which had an ogival nose made of aluminum, a cylindrical center section also made of aluminum, and a tapered afterbody made of fiber glass and plastic over a steel core.

The 60° delta vertical tail was made of 1/8-inch sheet steel and had an area equal to 0.683 of the wing area. The ventral fin had an area equal to two-thirds the vertical-tail area. The ratio of wing area and tail area to fuselage diameter was the same as for the model of reference 3. The V-tail arrangements tested were obtained by using two half-delta tails with the same area as the half-delta vertical tail. Because of space limitations the tail length for the present model was slightly less than that for the model of reference 3. All tail areas include that portion shielded by the fuselage.

TESTS AND CORRECTIONS

The tests were made in the Langley high-speed 7- by 10-foot tunnel through a Mach number range from 0.60 to 0.92 which corresponds to a Reynolds number from 4.5×10^6 to 5.0×10^6 based on the mean aerodynamic chord. The angle-of-attack range varied with loading conditions (the maximum range being from about -2° to 24°). Lateral parameter tests were made at angles of sideslip of $\pm 4^\circ$. Model normal force, axial force, side force, pitching moment, rolling moment, and yawing moment were indicated by means of an electrical strain-gage balance mounted internally in the fuselage.

Jet-boundary corrections have been applied to the data by the method of reference 4. Blockage corrections were applied to the data in

accordance with the method of reference 5, and corrections for the effect of longitudinal-pressure gradient over the model length have been applied.

Model support tares have not been applied except for a base-pressure adjustment. The adjusted data represent a condition of free-stream static pressure at the fuselage base.

The angles of attack and sideslip have been corrected for deflection of the sting support and balance system under load. No attempt has been made, however, to correct the data for distortion of the model under load.

RESULTS AND DISCUSSION

The aerodynamic characteristics in pitch of the model with 20° wing dihedral and various tail arrangements are presented in figure 5. The aerodynamic characteristics in pitch of the model with 50° wing dihedral and various tail arrangements are presented in figure 6. The variation of the lateral-stability parameters with angle of attack for the model with 20° wing dihedral and various tail arrangements is given in figure 7. The variation of the lateral-stability parameters with angle of attack for the model with 50° wing dihedral and various tail arrangements is shown in figure 8. The variation of $C_{n\beta}$ and $C_{l\beta}$ with Mach number is shown in figure 9.

Longitudinal Characteristics

Tests through the angle-of-attack range (figs. 5 and 6) indicate that the tail-off normal-force-curve slope $C_{N\alpha}$ varied with Mach number from 0.050 to 0.056 for 20° wing dihedral and from 0.039 to 0.046 for 50° wing dihedral. About two-thirds of the difference in normal-force-curve slope between the configuration with 20° wing dihedral and that with 50° wing dihedral can be attributed to a difference in projected planform area of the two configurations. Coefficients for both dihedral configurations are based on 0° wing dihedral which has a projected planform identical to that of a 60° delta wing. Addition of the V-tail configurations to both the 20° and 50° wing-dihedral configurations resulted in slight increases in normal-force-curve slope.

The 20° wing-dihedral configuration with tail off was generally longitudinally stable for the α and Mach number ranges tested. The 50° wing-dihedral configuration with tail off had a region of instability at high angles of attack at $M = 0.80$ and possibly above $M = 0.80$. The variation of pitching moment for both configurations was similar to that obtained at low speed (ref. 3). The tail configurations were primarily

selected to provide lateral stability. However, a brief discussion of their effect on longitudinal stability is included herein. Addition of the half-delta vertical tail resulted generally in little change in the variation of pitching-moment coefficient with α except for the $\Gamma_w = 50^\circ$ configuration where a slight instability is noted near $\alpha = 17^\circ$.

The 30° V-tail and the 30° V-tail-plus-ventral-fin configurations tested with 20° wing dihedral resulted in slight increases in longitudinal stability except for a region of about neutral stability in the vicinity of $\alpha = 15^\circ$. The 45° V-tail tested with the 50° wing dihedral angle resulted in a large increase in stability with a generally linear variation of pitching-moment coefficient with angle of attack; this increase eliminated the unstable break near $\alpha = 17^\circ$.

Lateral Characteristics

Lateral-parameter tests at $\pm 4^\circ$ angle of sideslip have been made through the angle-of-attack and Mach number ranges for both the 20° and 50° wing dihedral angles (figs. 7 and 8). Tests made through the sideslip-angle range in reference 3 indicated generally linear variations. Therefore, lateral-parameter tests have been restricted to $\beta = \pm 4^\circ$. The data of figure 7 indicate that the 20° wing-dihedral configuration with tail off is directionally unstable throughout the angle-of-attack and Mach number ranges tested. However, the instability was about constant with only slight variations at high α being noted. Addition of the half-delta vertical tail provided a stabilizing increment in $C_{n\beta}$

which resulted in a stable configuration except at the highest angles of attack where the half-delta vertical-tail contribution decreased. This trend is similar to that found in low-speed tests of this configuration (ref. 3) which show large decreases in directional stability above 22° angle of attack and also in tests of a 45° delta wing using a similar fuselage (ref. 6). This large decrease in directional stability is probably associated with an unfavorable sidewash from the wing-fuselage combination which reduced the tail effectiveness at the higher angles of attack.

The model with a 30° V-tail was directionally stable up to an angle of attack of about 12° . Above 12° the model became directionally unstable, but the instability tended to reduce with increasing angle of attack with the model becoming stable again at angles of attack of about 20° . The addition of the ventral fin gave an almost constant increment of stability throughout the angle-of-attack and Mach number ranges investigated and resulted in directional stability for the 30° V-tail plus ventral of about the same magnitude as that of the half-delta vertical-tail configuration.

The data of figure 8 indicate that the 50° wing-dihedral configuration with tail off is slightly directionally unstable at low angles of attack.

As the angle of attack is increased, the directional instability decreases until above 10° angle of attack the configuration becomes stable. This variation probably can be attributed to the increase in lateral area of the wing behind the center of moments at the higher wing dihedral angle. Addition of the half-delta vertical tail to the $\Gamma_w = 50^\circ$ wing-fuselage combination results in a stable configuration through most of the angle-of-attack and Mach number ranges tested. The favorable increment of C_{n_β} contributed by the tail decreases at the higher test angles of attack and reverses at the highest test α , which results in an unstable configuration. The stable increment in C_{n_β} due to adding the vertical tail in this case was only about one-half the increment obtained by adding the vertical tail to the 20° wing configuration (fig. 7). The model with the -45° V-tail was directionally stable for all angles of attack and Mach numbers tested, as was found in the low-speed tests of reference 3 for a similar configuration. However, a slight reduction in directional stability occurred between $\alpha = 12^\circ$ and 16° .

The tail-off effective dihedral for the model with 20° wing dihedral was negative ($+C_{l_\beta}$) at $\alpha = 0^\circ$; however, C_{l_β} varies with α so that the dihedral effect is positive ($-C_{l_\beta}$) for angles of attack above about 5° . The positive effective dihedral increases with angle of attack up to about 12° , above which the variation of effective dihedral with α is somewhat erratic with a general tendency to decrease. The addition of the tail configuration to the 20° wing-dihedral configuration generally resulted in an increase in positive dihedral effect with little change in the variation of C_{l_β} with α . For all tail configurations tested the effective dihedral was slightly negative at $\alpha = 0^\circ$ and positive over most of the positive range of α tested.

The data for the 50° wing-dihedral configurations with tail off (fig. 8) indicate that increasing the wing dihedral from 20° to 50° contributed a positive increment of effective dihedral as expected, which resulted in $-C_{l_\beta}$ over the test range. As the angle of attack is increased, the positive effective dihedral increases until about $\alpha = 12^\circ$; above $\alpha = 12^\circ$ there was a fairly rapid reduction in effective dihedral. Addition of the half-delta vertical tail shifted the effective dihedral in a positive direction but had little effect on the variation of C_{l_β} with α . The -45° delta V-tail shifted the effective dihedral in a negative direction, and this shift together with the variation with angle of attack resulted in the model having a slightly negative dihedral effect at high angles of attack at $M = 0.80$, and possibly at other Mach numbers above $M = 0.80$.

The tail-off data of figure 9 indicate that the directional instability at $\alpha = 0^\circ$ decreased slightly with increase in Mach number up to $M = 0.60$ for both the 20° and 50° wing-dihedral configurations and remained generally constant above $M = 0.60$. The effective dihedral showed a change in a negative direction with increasing Mach number up to about $M = 0.60$ and generally remained constant above $M = 0.60$ for both the 20° and 50° wing-dihedral configurations.

CONCLUSIONS

An investigation at high subsonic speeds was made in the Langley high-speed 7- by 10-foot tunnel to determine the static stability characteristics of a cambered-delta-wing model with wing dihedral angles of 20° and 50° and with various tail configurations. The results indicated the following conclusions:

1. The 20° wing-dihedral configuration with tail off was generally longitudinally stable through the angle-of-attack range tested for all Mach numbers. The 50° wing-dihedral configuration was generally longitudinally stable except for a range of neutral stability near an angle of attack of 17° at a Mach number of 0.80 and possibly above this Mach number.

2. The 20° wing-dihedral configuration with tail off was directionally unstable throughout the angle-of-attack range for all Mach numbers. The 50° wing-dihedral configuration with tail off was directionally unstable at low angles of attack but became directionally stable at high angles of attack.

3. The tail-off effective dihedral was negative for the 20° wing-dihedral configuration at low angles of attack but increased with increasing angle of attack until the configuration had positive effective dihedral above about an angle of attack of 5° . Increasing the wing dihedral from 20° to 50° increased the positive effective dihedral so that the configuration had positive effective dihedral throughout the angle-of-attack range tested.

4. Addition of the half-delta vertical tail to either configuration resulted in a stable increment of directional stability at low angles of attack but a loss in tail effectiveness with increasing angle of attack resulted in directional instability for some configurations in the high angle-of-attack range. The 20° wing-dihedral configuration with 30° V-tail plus ventral fin resulted in a directionally stable configuration throughout the angle-of-attack and Mach number ranges tested. The 45° V-tail with the 50° wing-dihedral configuration was directionally stable

for angles of attack and Mach numbers tested. However, large reductions in positive effective dihedral occurred for the 50° wing-dihedral configuration at the higher angles of attack.

Langley Aeronautical Laboratory,
National Advisory Committee for Aeronautics,
Langley Field, Va., August 8, 1956.

REFERENCES

1. Paulson, John W.: Comparison of the Static Stability of a 68.7° Delta-Wing Model With Dihedral and a Twisted and Cambered Wing Model of the Same Plan Form. NACA RM L55B11, 1955.
2. Fisher, Lewis R.: Low-Speed Static Longitudinal and Lateral Stability Characteristics of Two Low-Aspect-Ratio Wings Cambered and Twisted To Provide a Uniform Load at a Supersonic Flight Condition. NACA RM L51C20, 1951.
3. Riebe, John M., and Moseley, William C., Jr.: Low-Speed Static Stability Characteristics of a Cambered-Delta-Wing Model. NACA RM L55L21a, 1955.
4. Gillis, Clarence L., Polhamus, Edward C., and Gray, Joseph L., Jr.: Charts for Determining Jet-Boundary Corrections for Complete Models in 7- by 10-Foot Closed Rectangular Wind Tunnels. NACA WR L-123, 1945. (Formerly NACA ARR L5G31.)
5. Herriot, John G.: Blockage Corrections for Three-Dimensional-Flow Closed-Throat Wind Tunnels, With Consideration of the Effect of Compressibility. NACA Rep. 995, 1950. (Supersedes NACA RM A7B28.)
6. Few, Albert G., Jr.: Investigation at High Subsonic Speeds of the Static Lateral and Directional Stability and Tail-Loads Characteristics of a Model Having a Highly Tapered Swept Wing of Aspect Ratio 3 and Two Horizontal-Tail Positions. NACA RM L56E29, 1956.

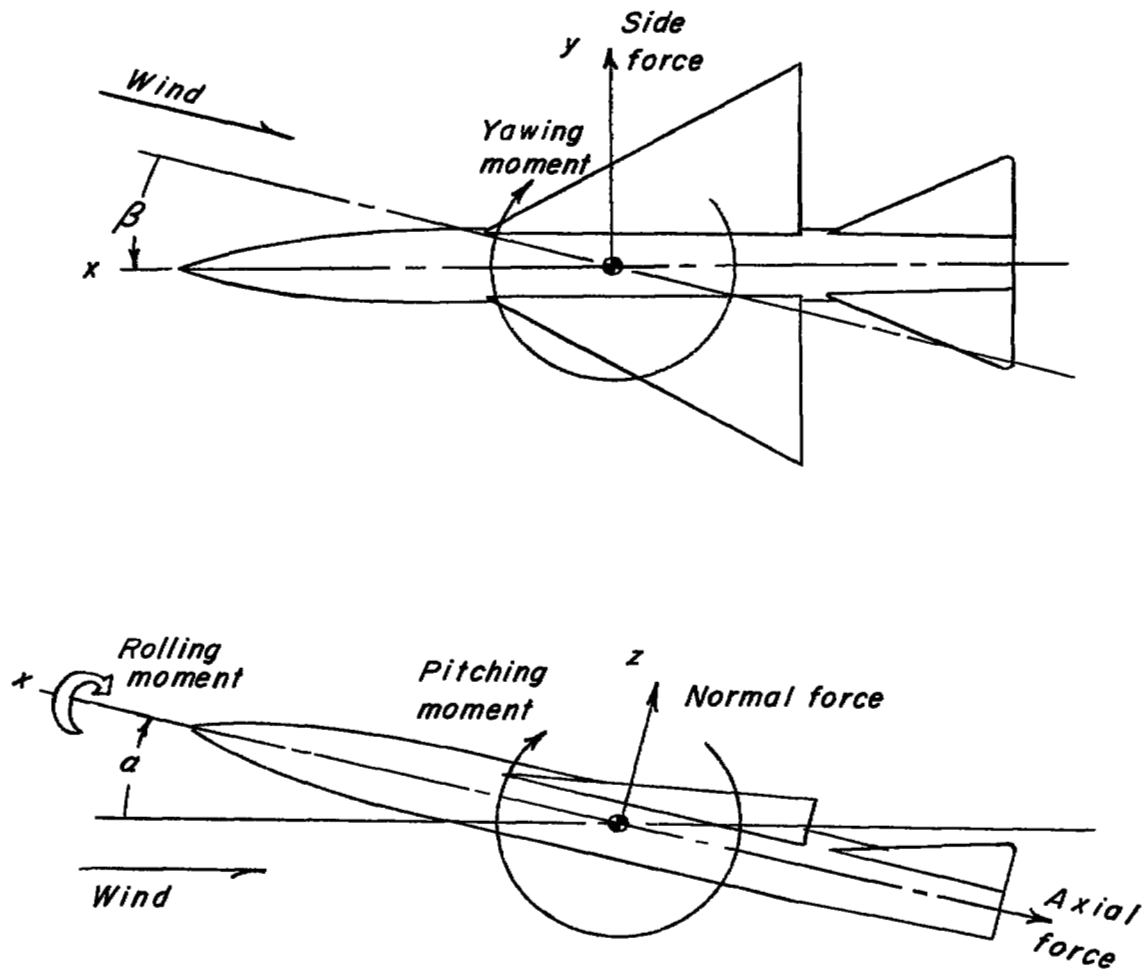


Figure 1.- System of axes used. Positive directions of forces, moments, and angles are indicated by arrows.

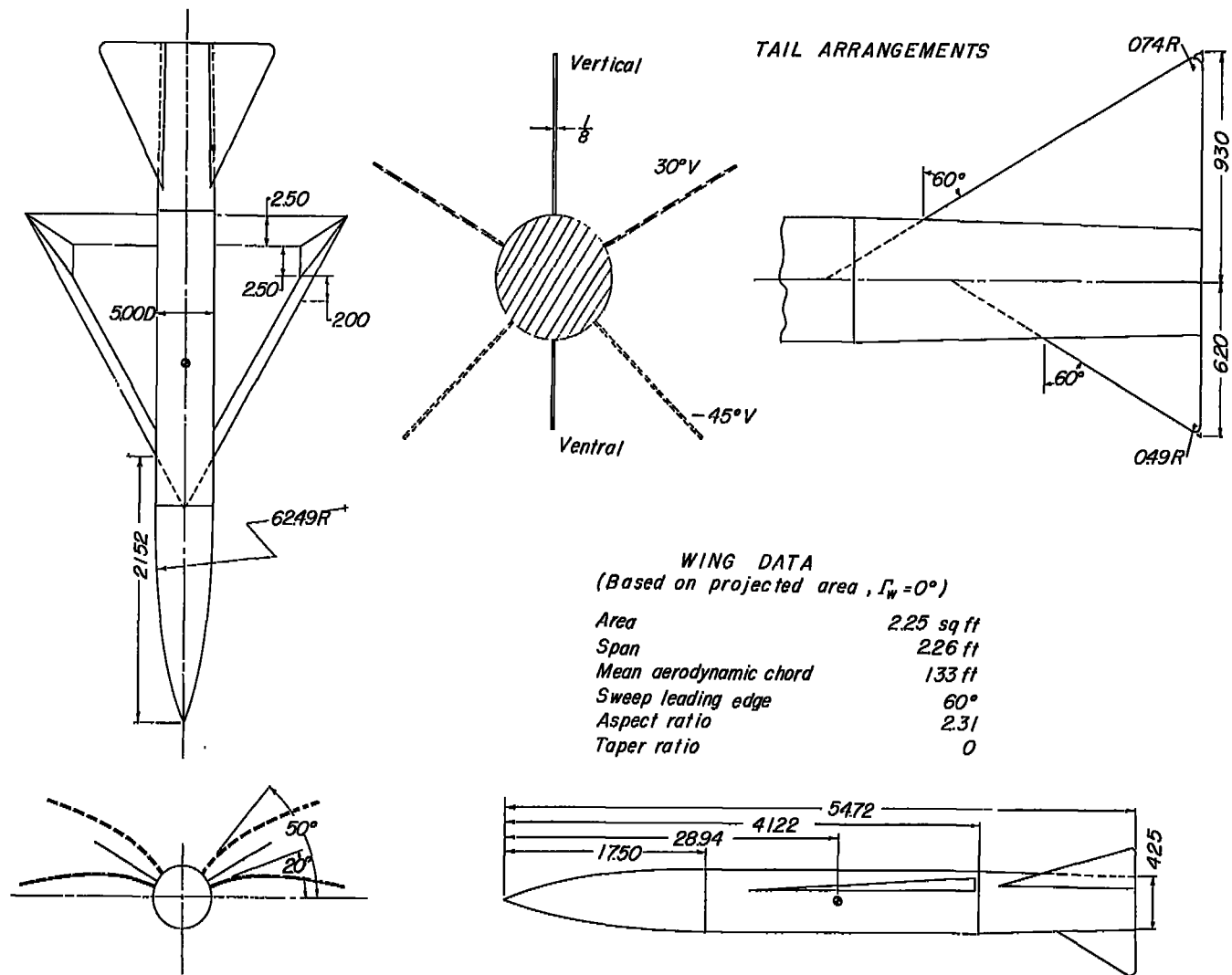


Figure 2.- Details of test model. (Dimensions are in inches unless otherwise noted.)



Figure 3.- Test model mounted on sting in tunnel.

L-90226



Figure 3.- Concluded.

L-90227

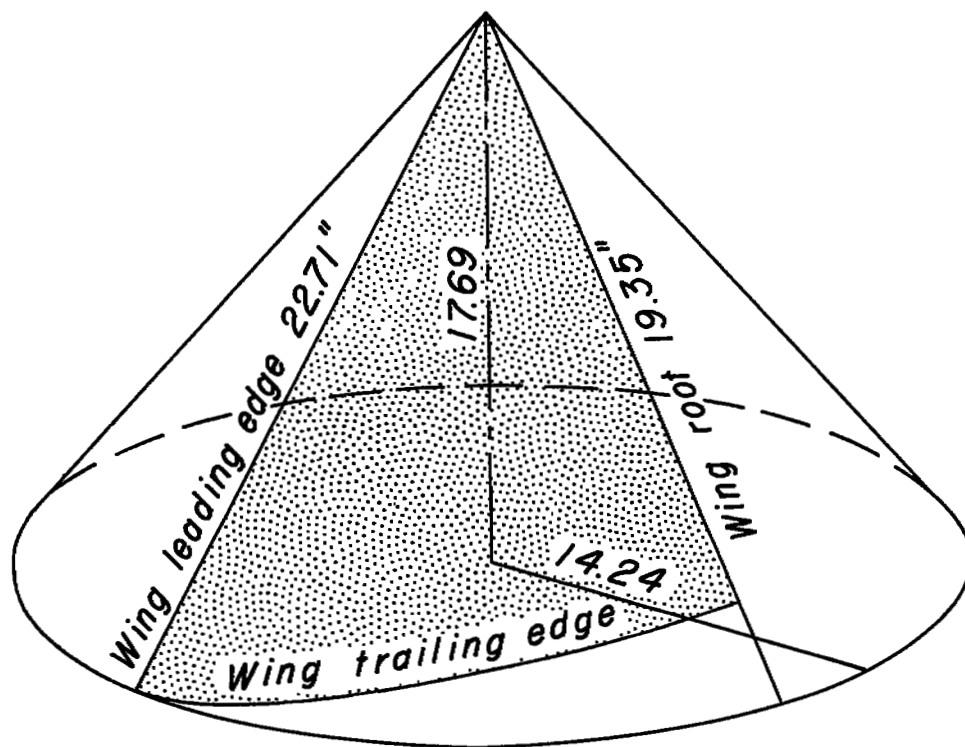
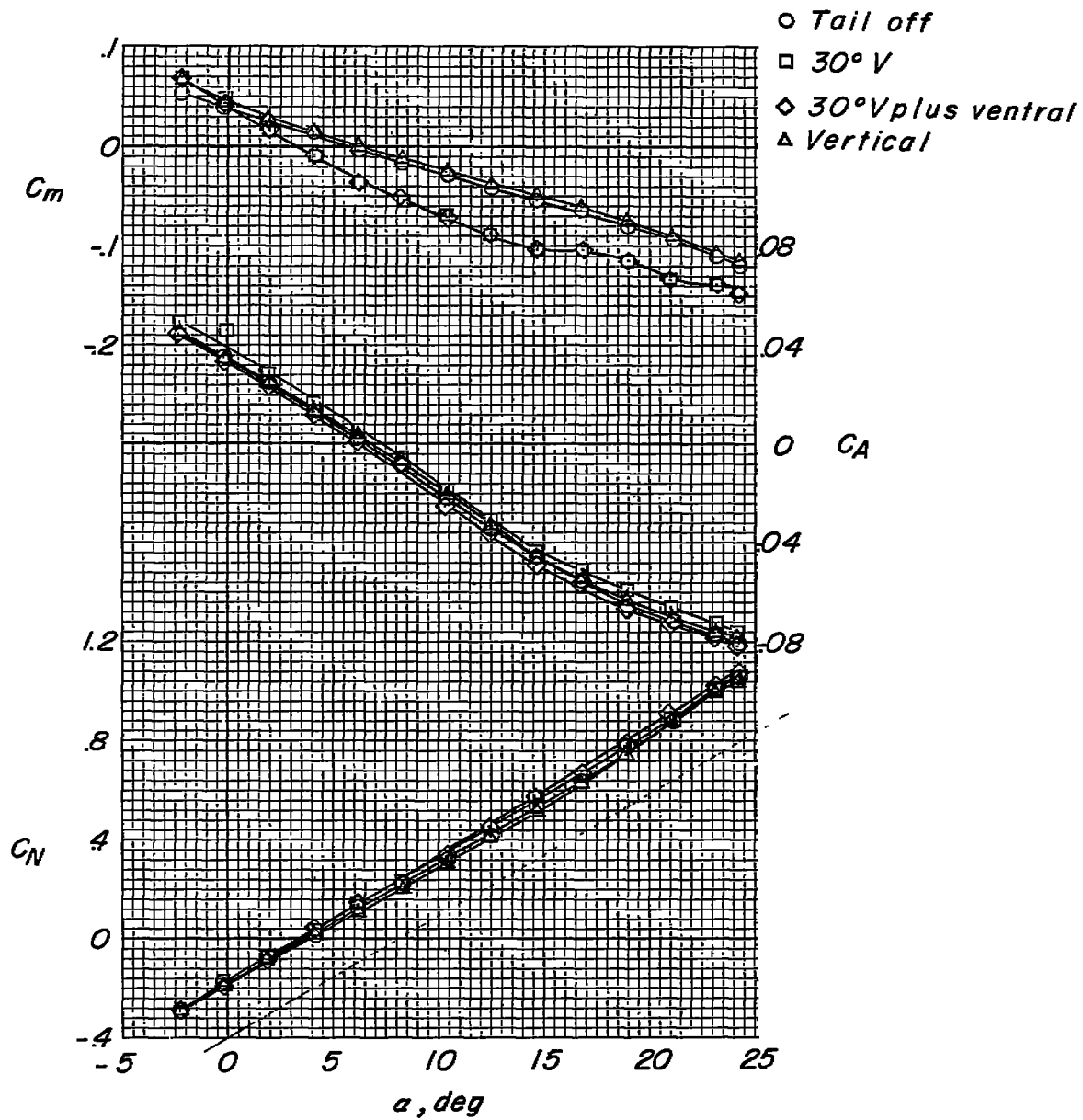


Figure 4.- Sketch showing development of cambered delta wing.



(a) $M = 0.60$.

Figure 5.- Aerodynamic characteristics in pitch of the model with 20° wing dihedral.

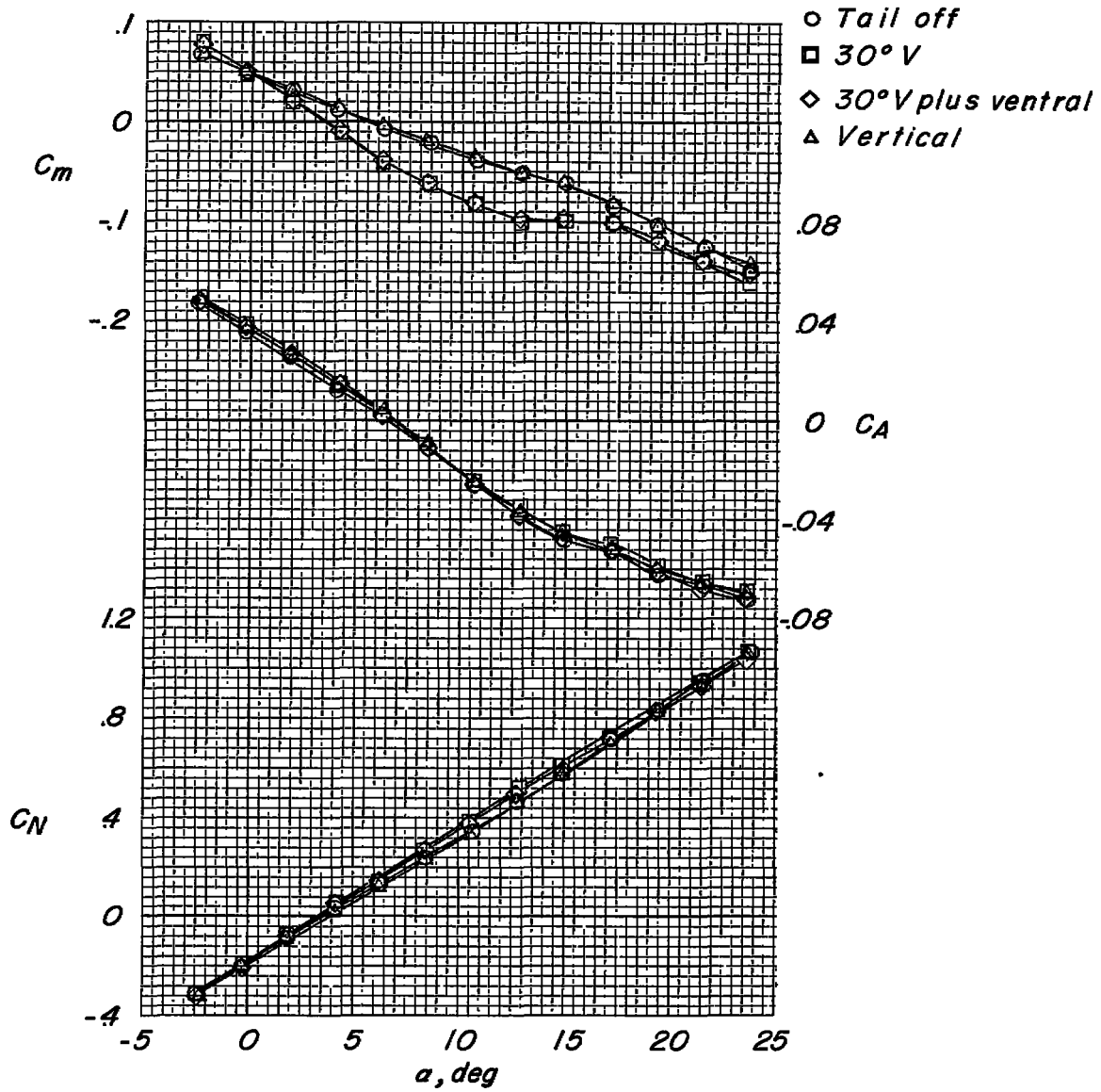
(b) $M = 0.80$.

Figure 5.- Continued.

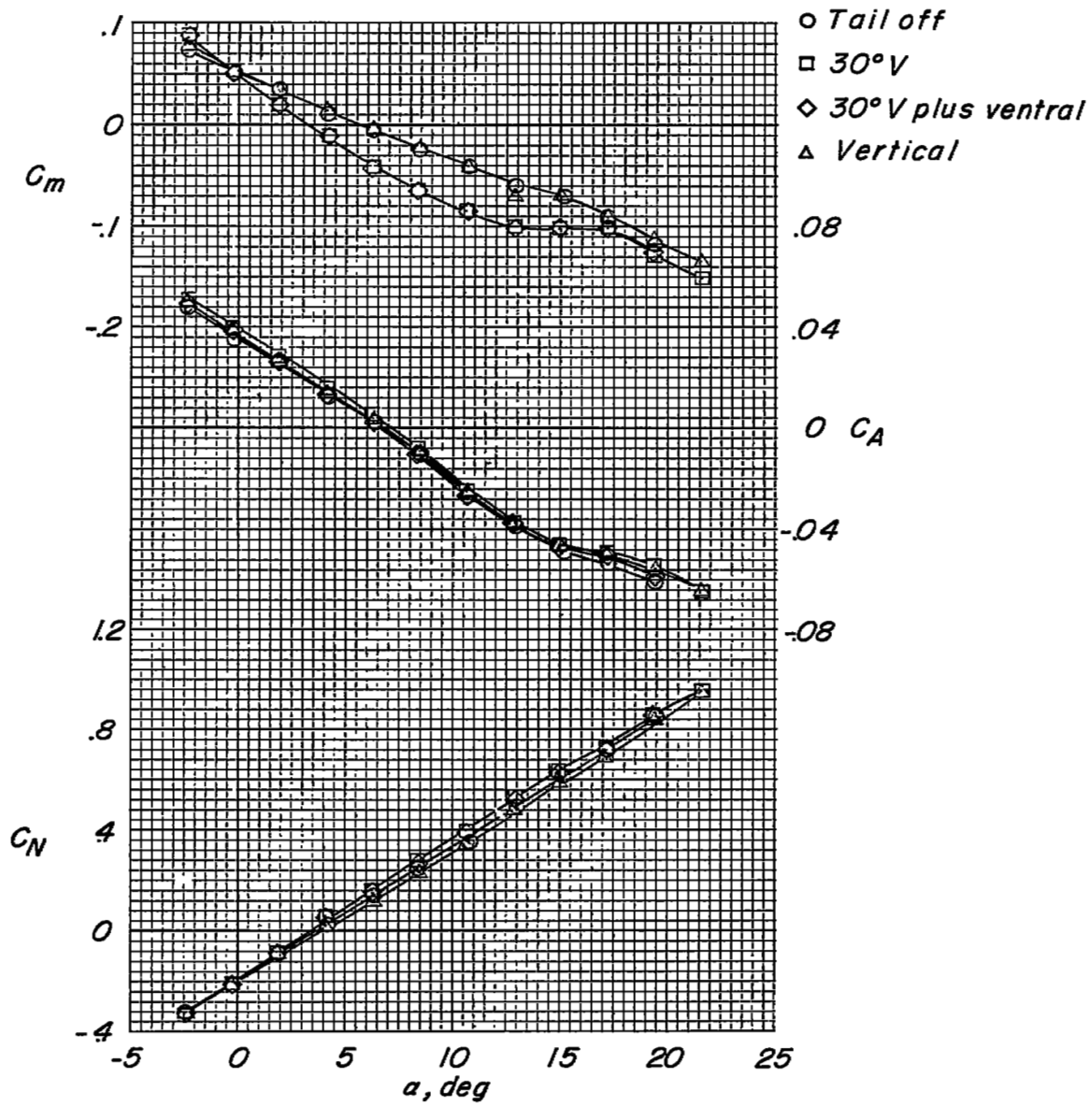
(c) $M = 0.85$.

Figure 5.- Continued.

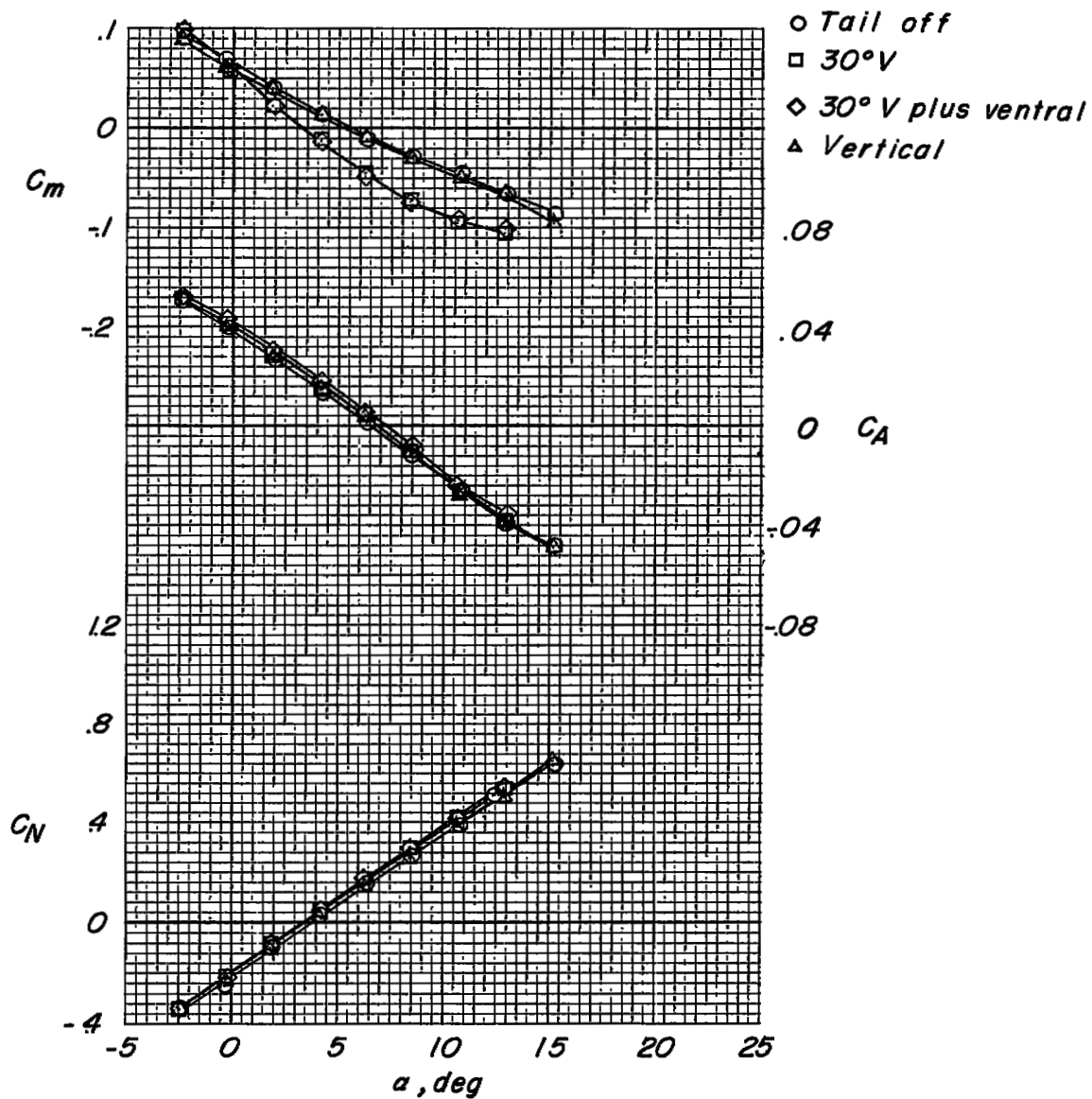
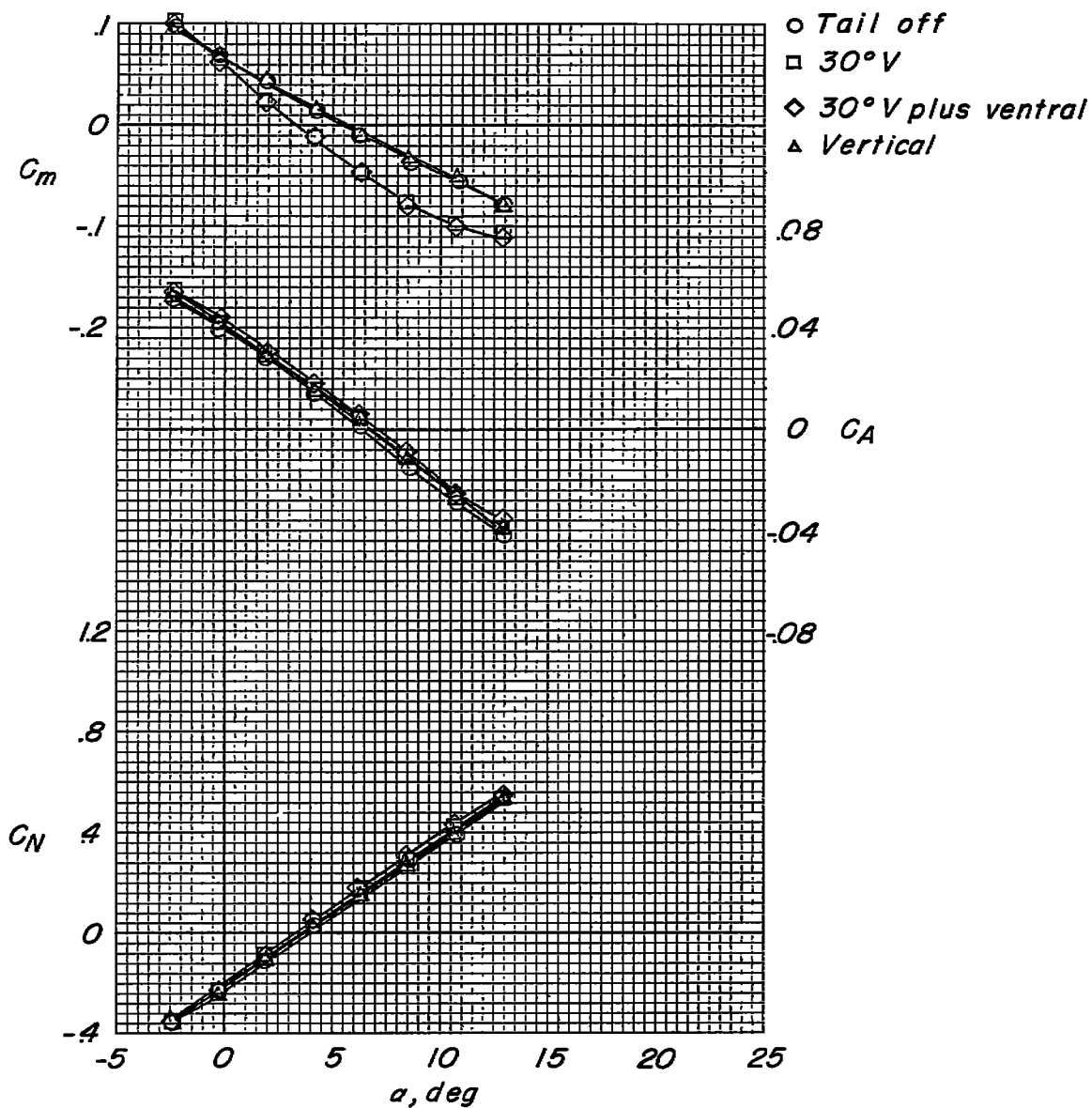
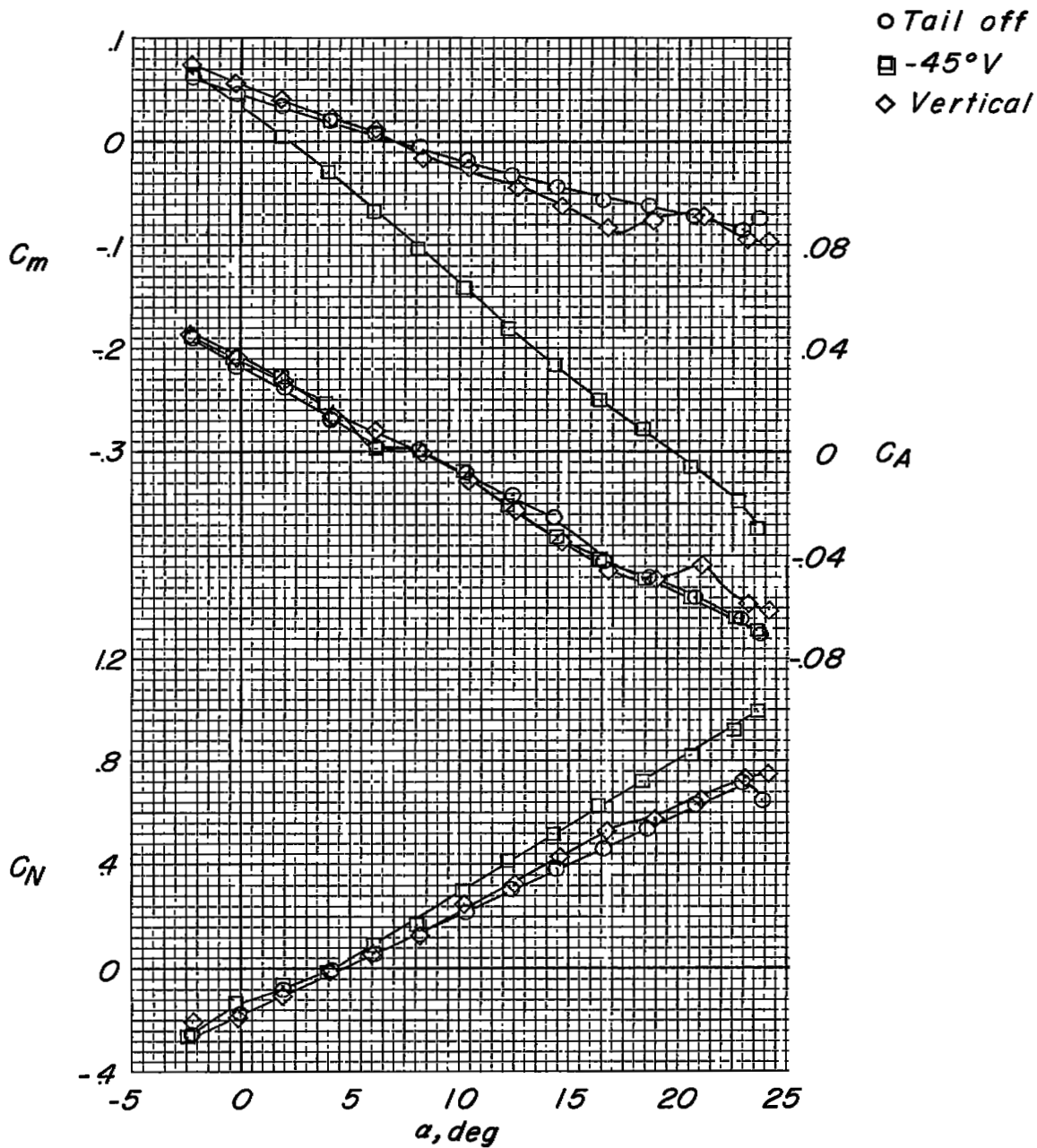
(d) $M = 0.90$.

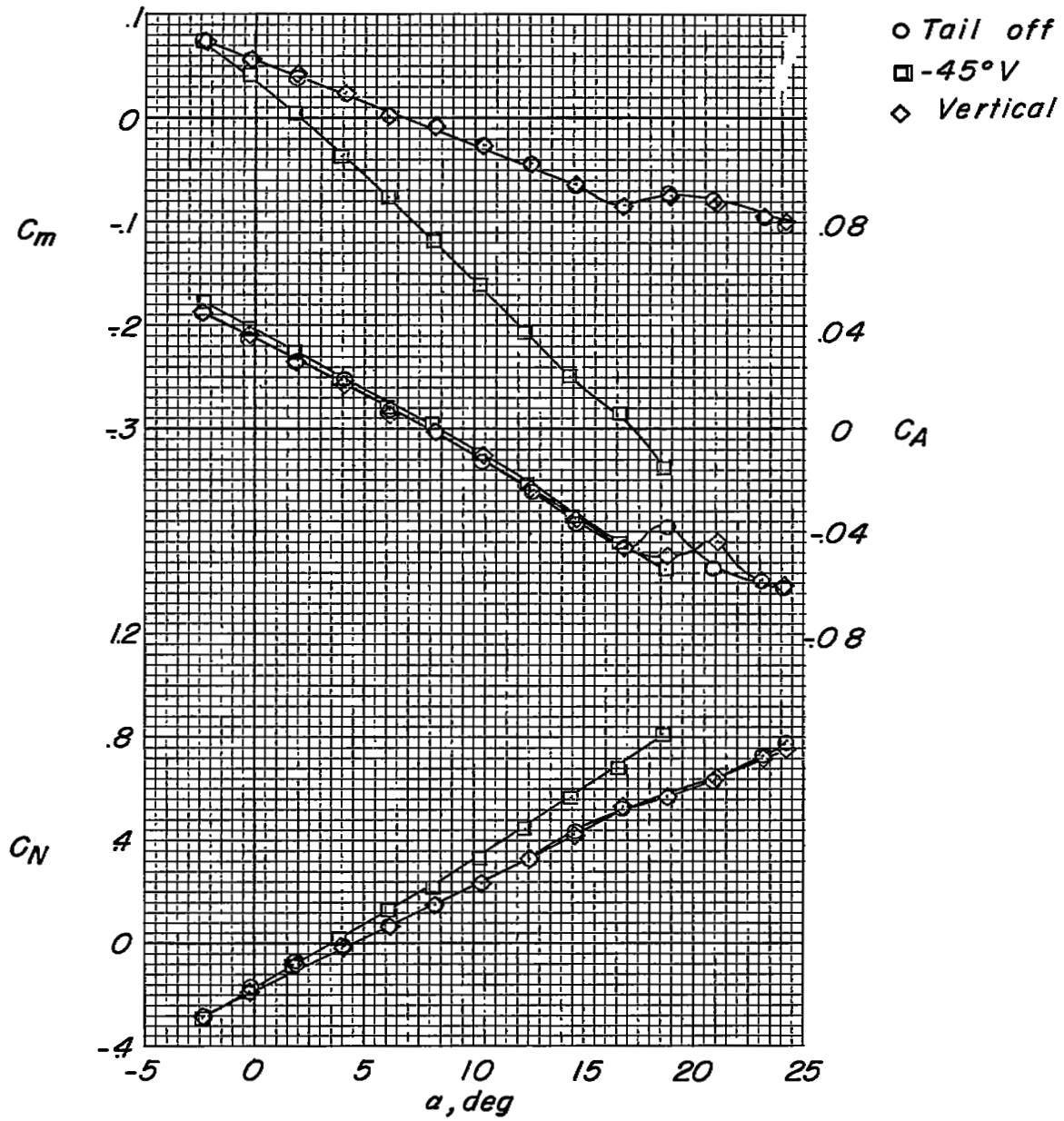
Figure 5.- Continued.



(e) $M = 0.92$.

Figure 5.- Concluded.

(a) $M = 0.60$.Figure 6.- Aerodynamic characteristics in pitch of the model with 50° wing dihedral.



(b) $M = 0.80$.

Figure 6.- Continued.

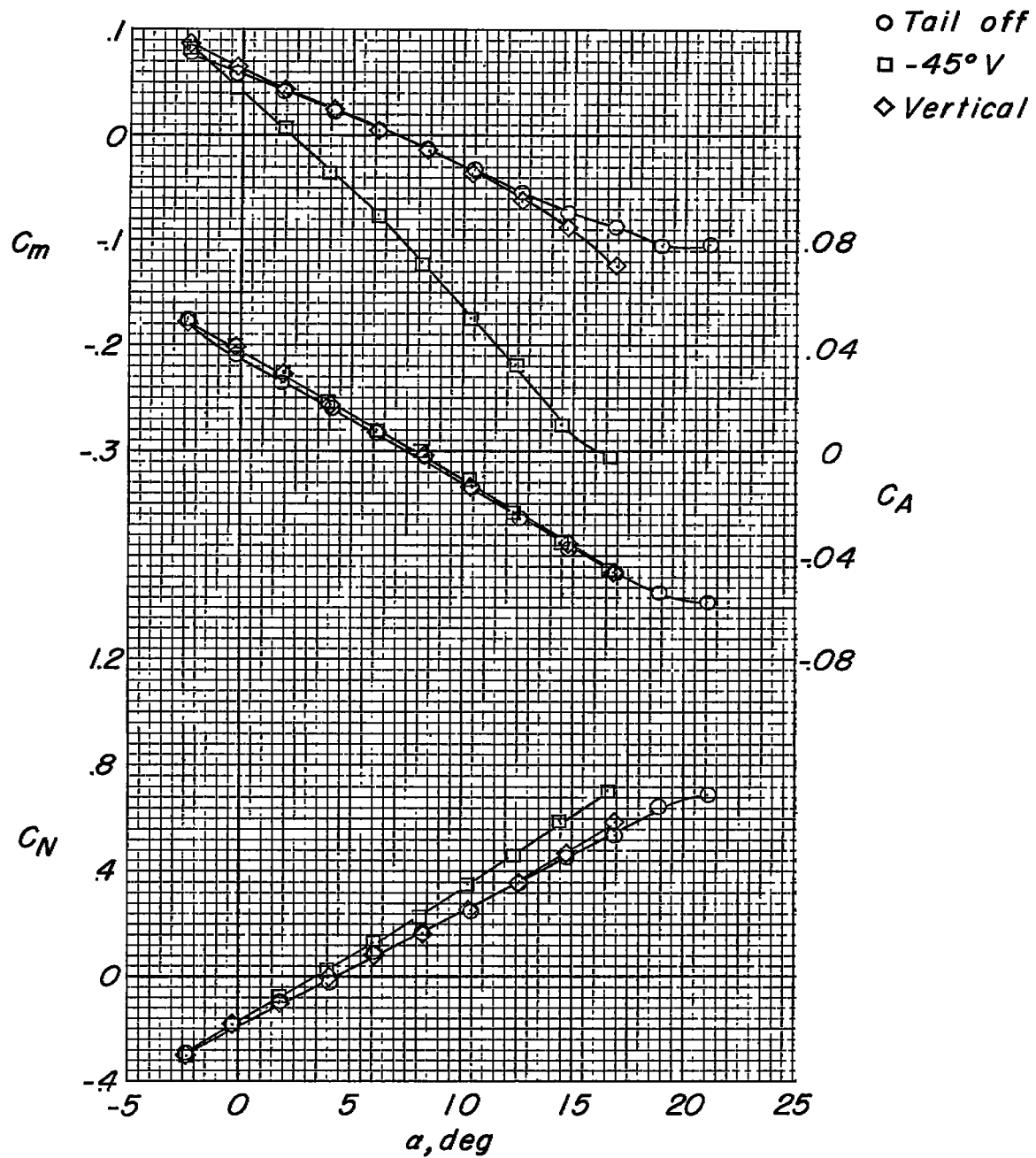
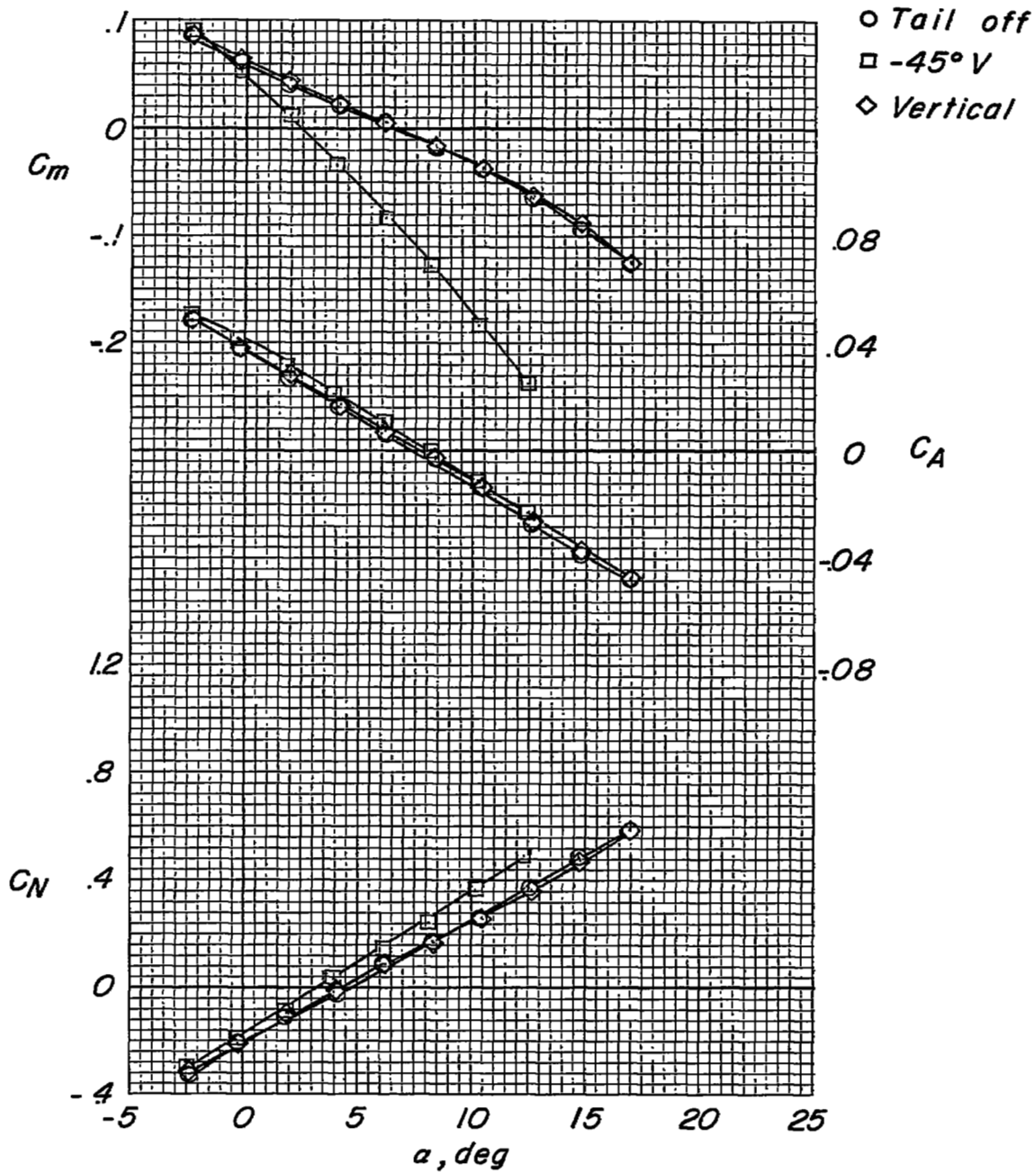
(c) $M = 0.85$.

Figure 6.- Continued.



(d) $M = 0.90$.

Figure 6.- Continued.

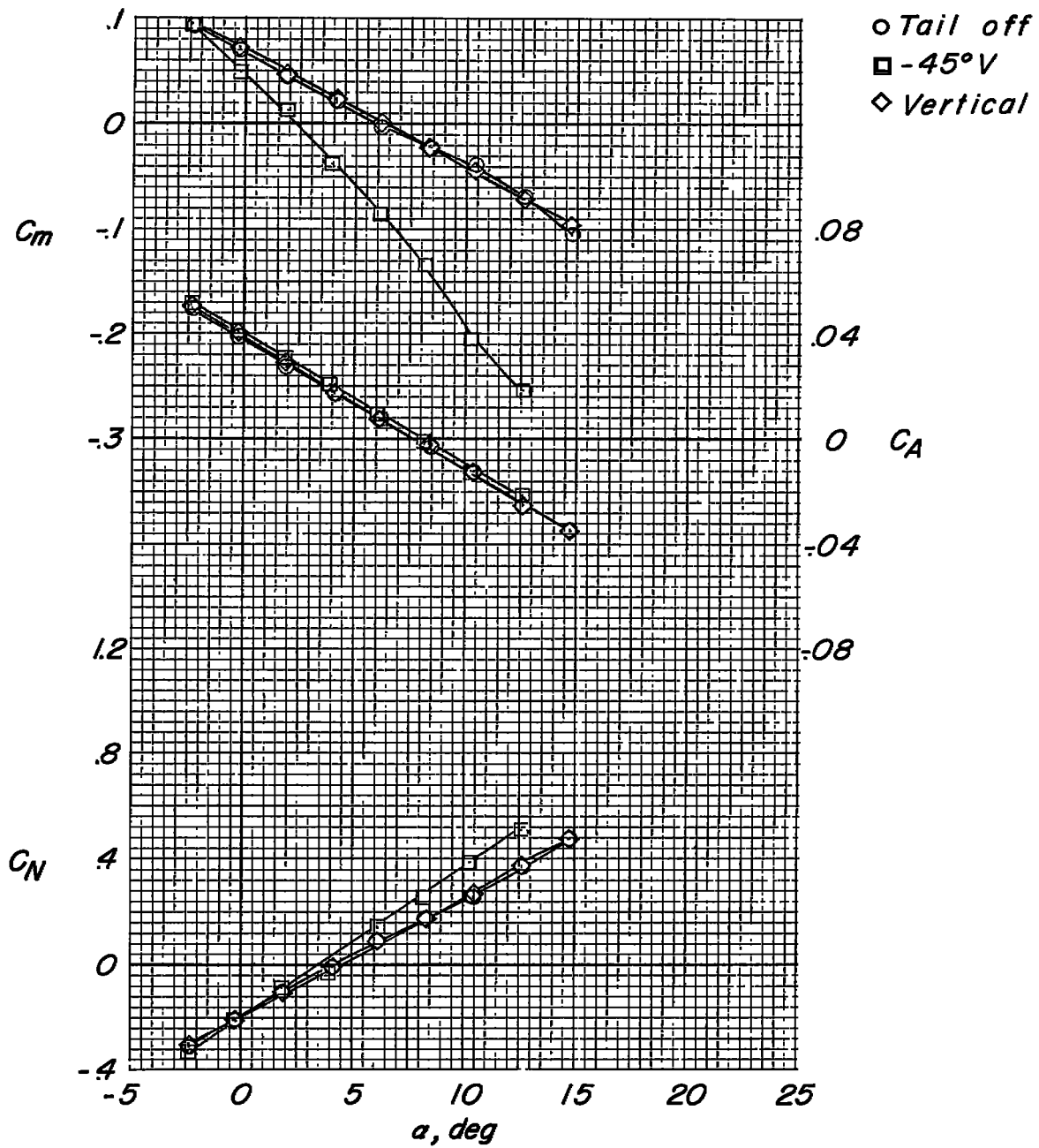
(e) $M = 0.92$.

Figure 6.- Concluded.

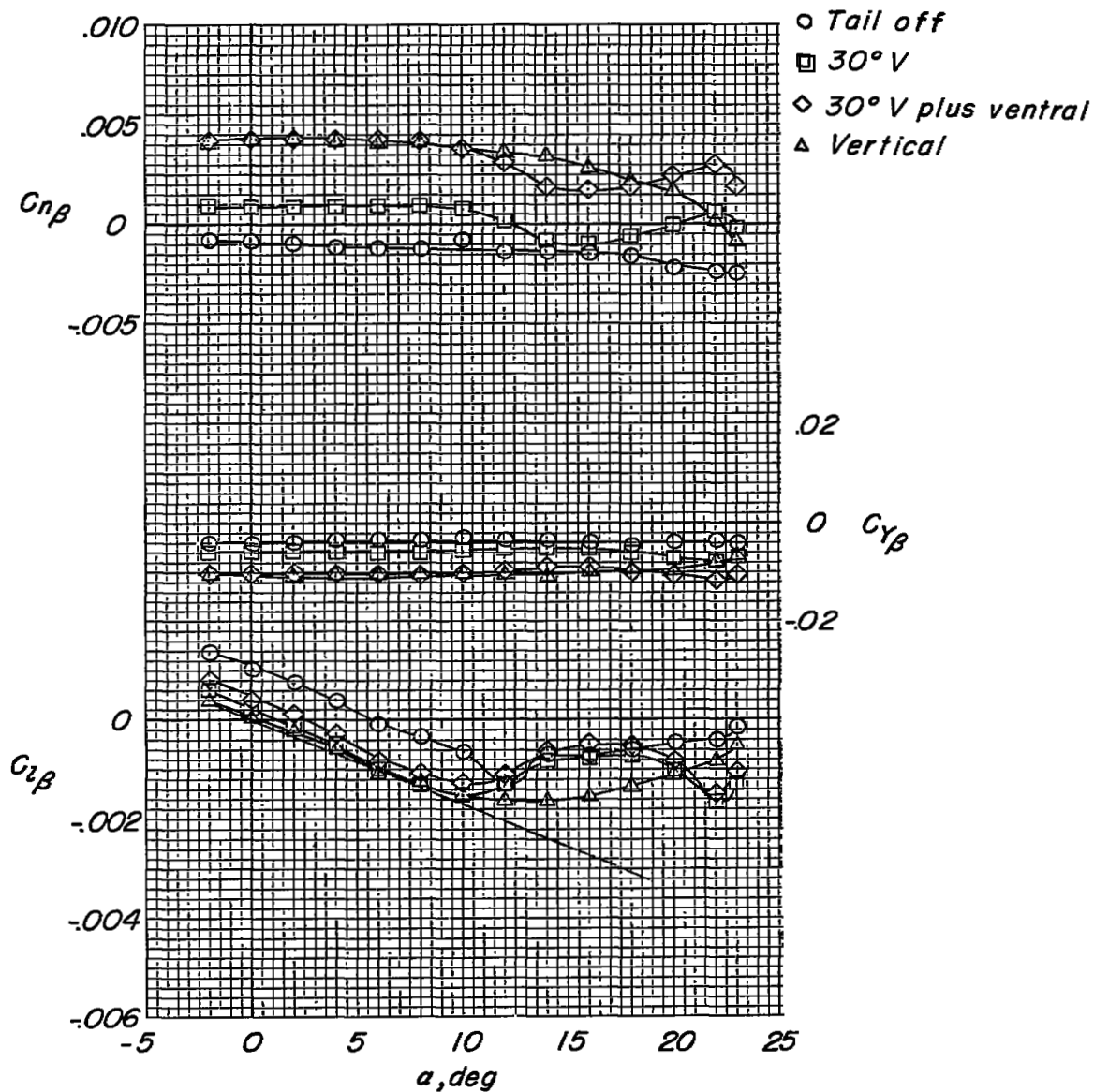
(a) $M = 0.60$.

Figure 7.- Variation of lateral-stability parameters with angle of attack for model with 20° wing dihedral.

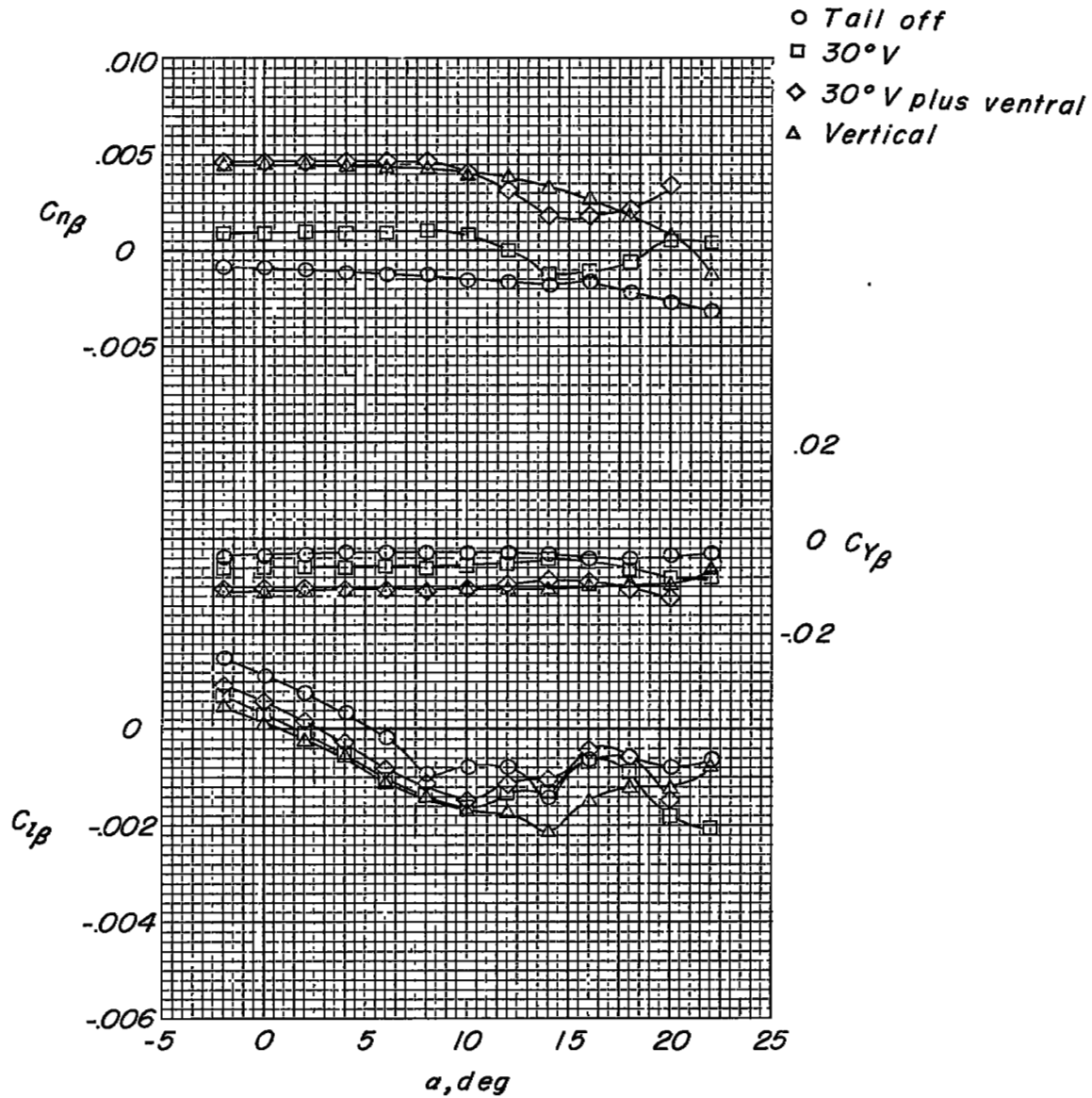
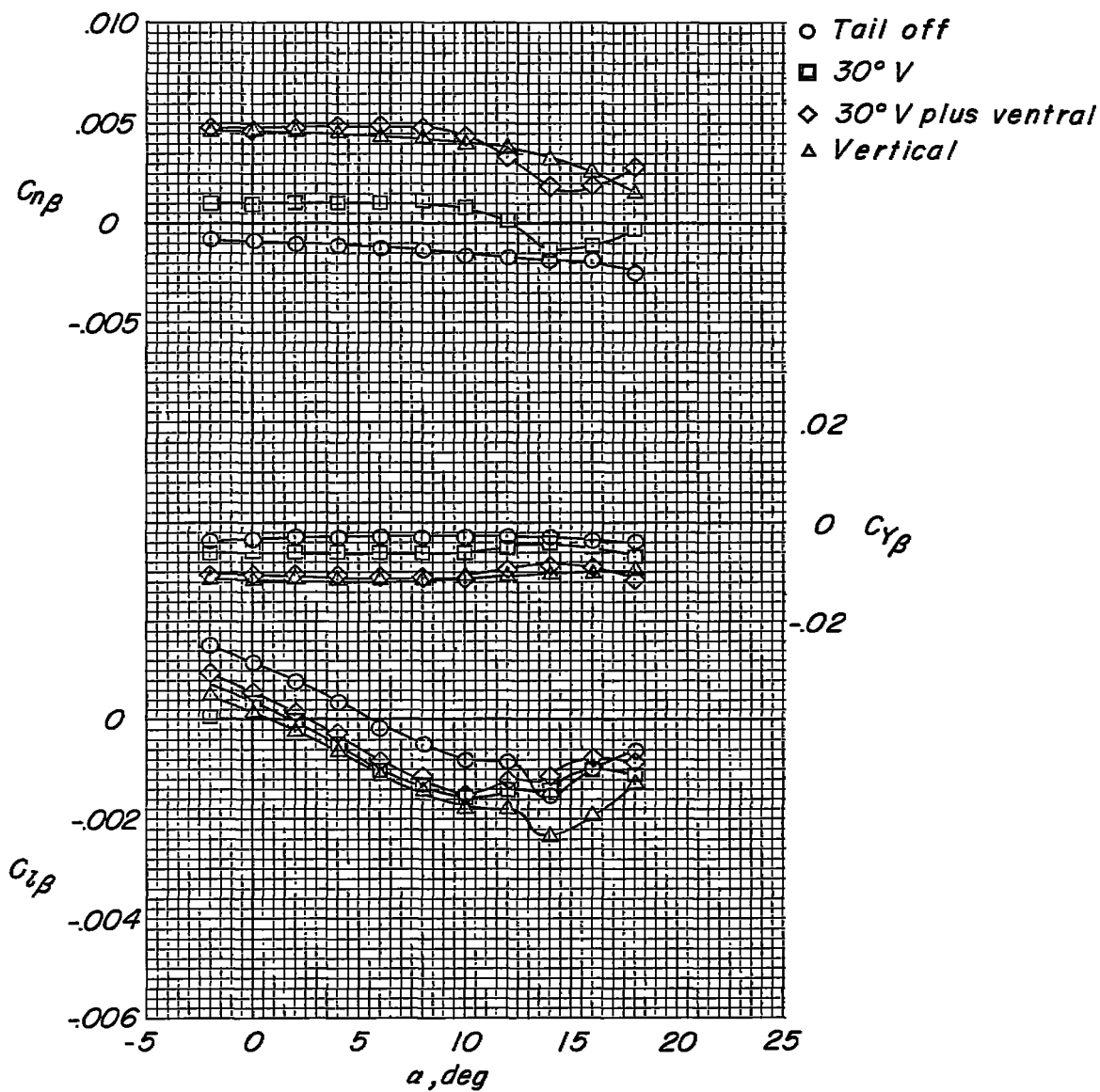
(b) $M = 0.80$.

Figure 7.- Continued.



(c) $M = 0.85$.

Figure 7.- Continued.

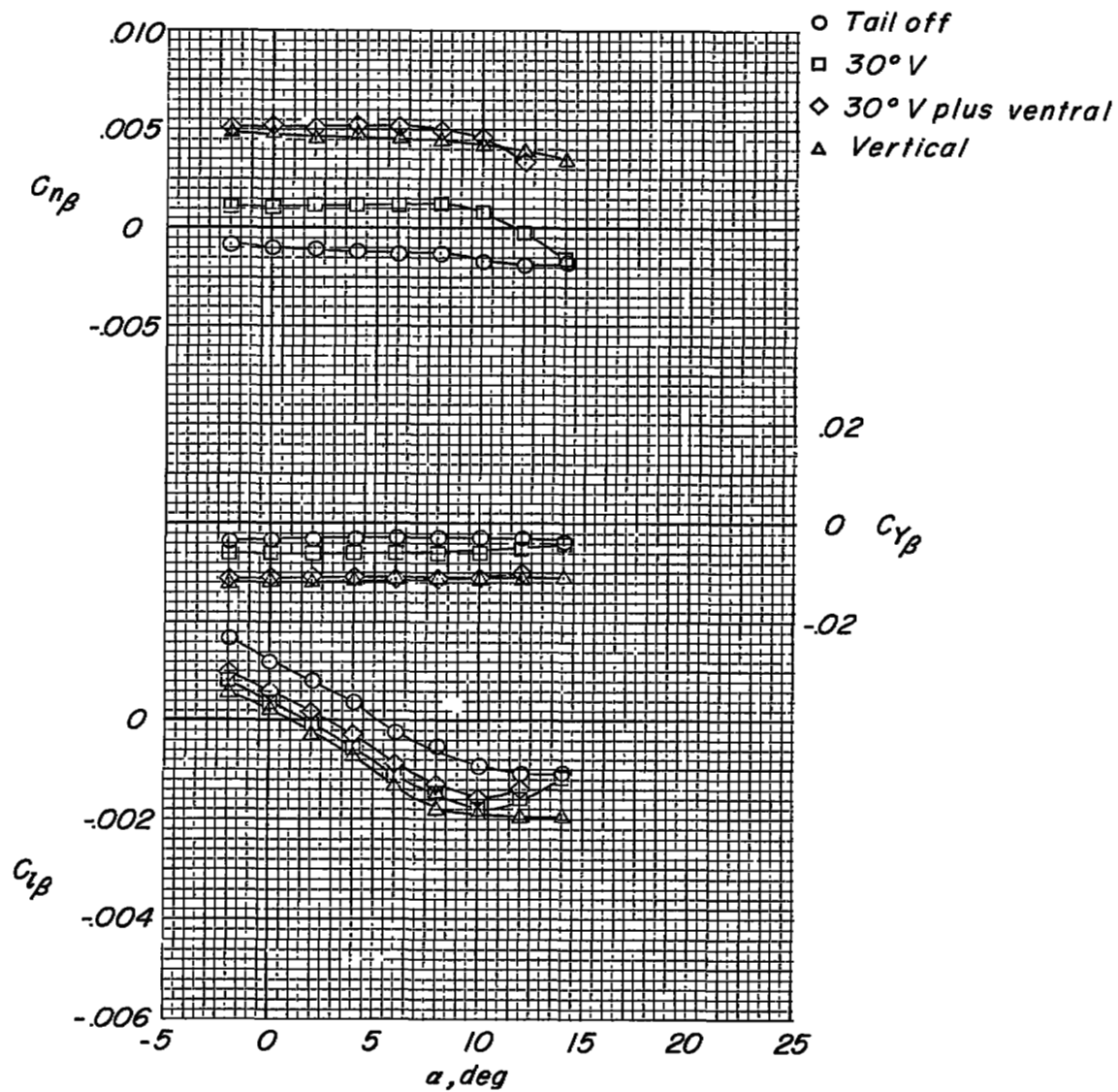
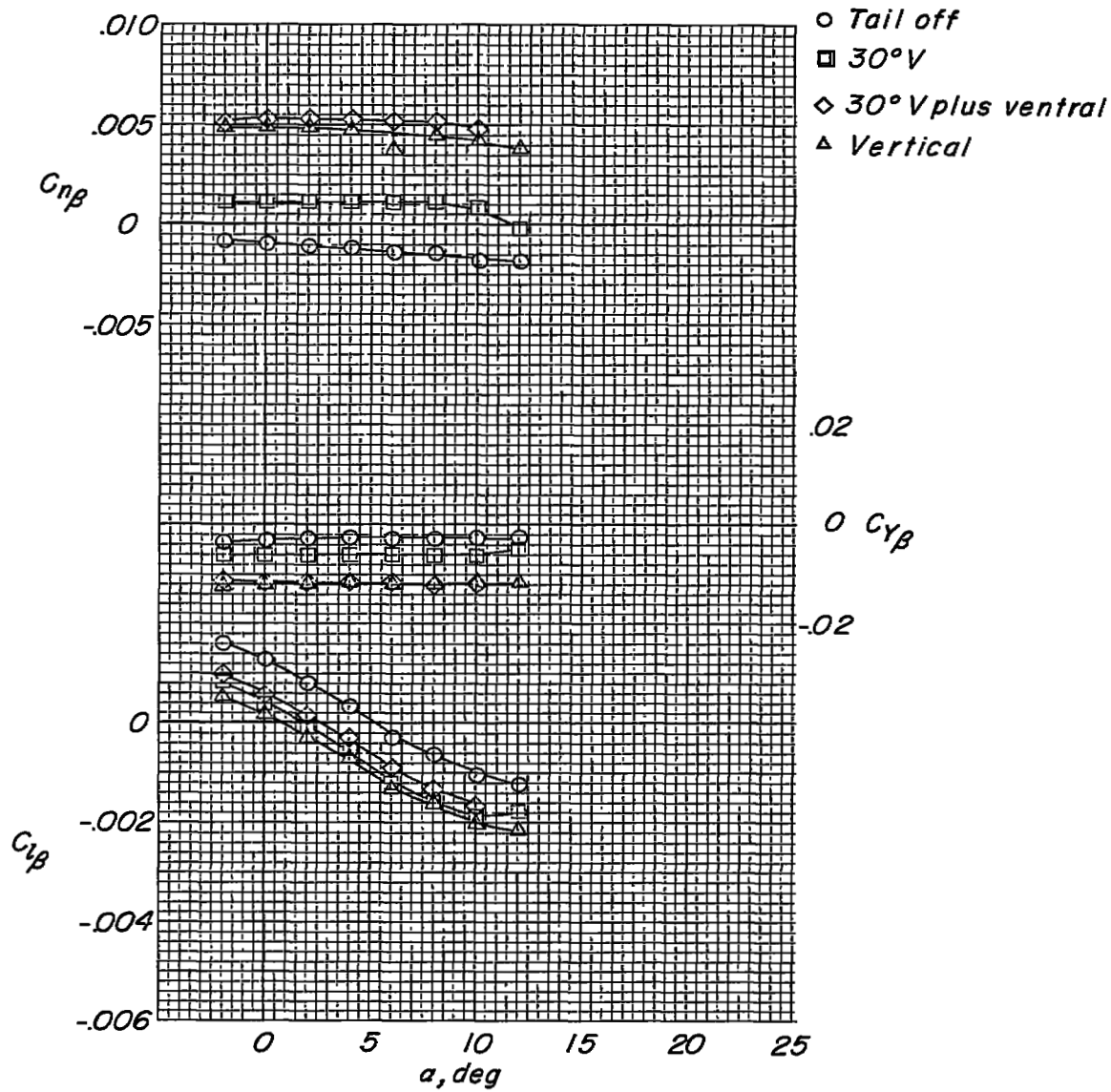
(d) $M = 0.90$.

Figure 7.- Continued.



(e) $M = 0.92$.

Figure 7.- Concluded.

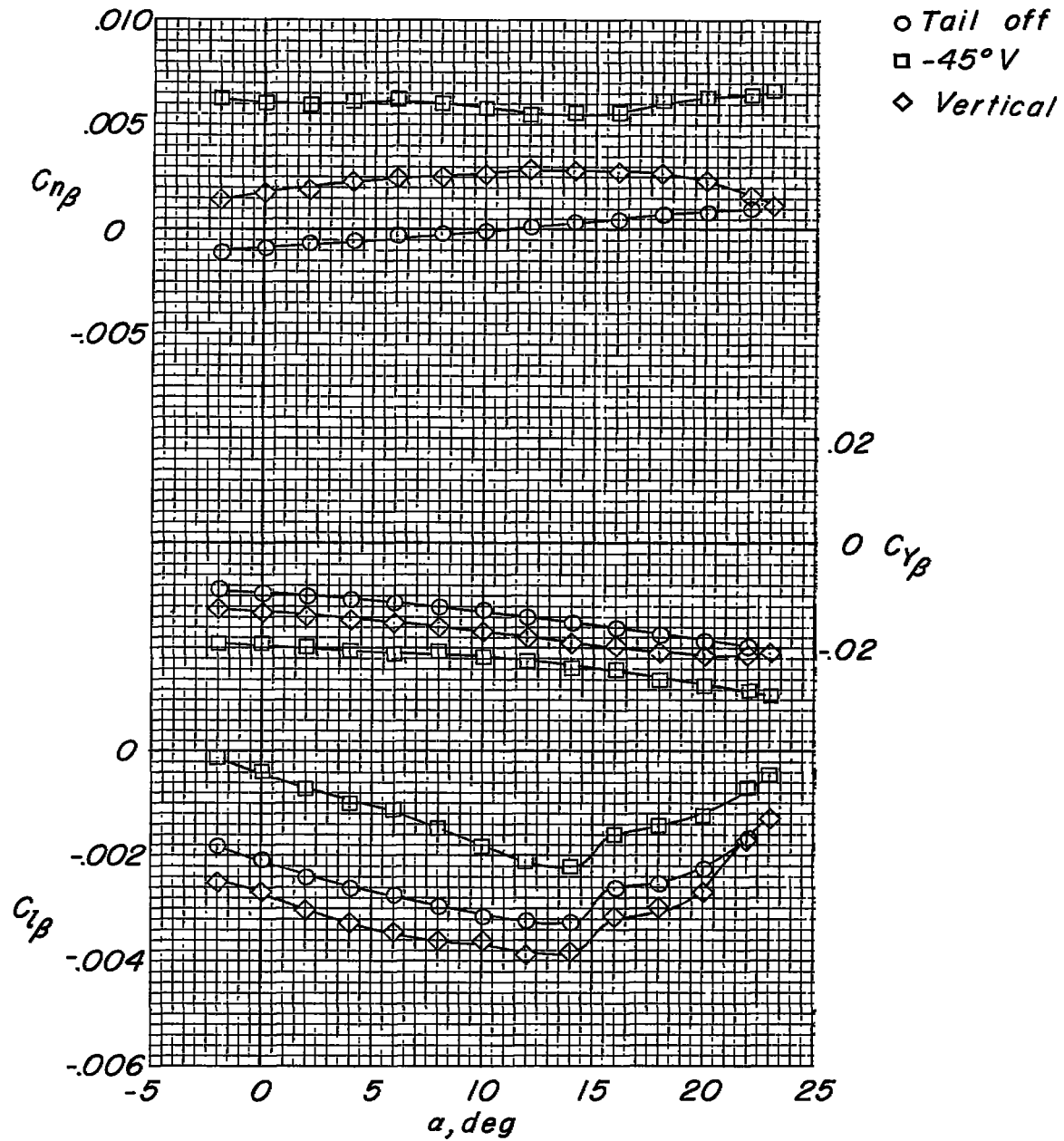
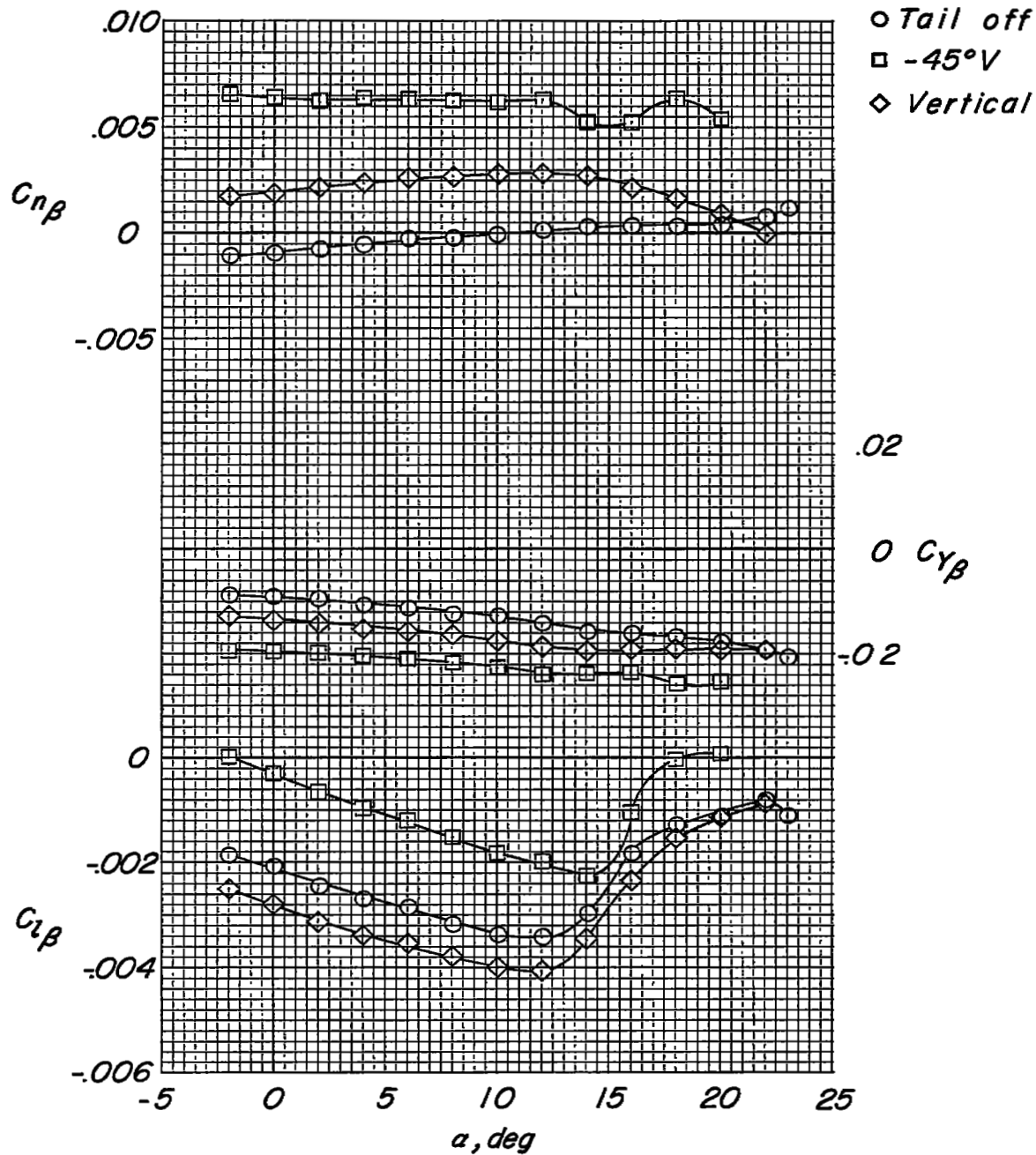
(a) $M = 0.60$.

Figure 8.- Variation of lateral-stability parameters with angle of attack for model with 50° wing dihedral.



(b) $M = 0.80$.

Figure 8.- Continued.

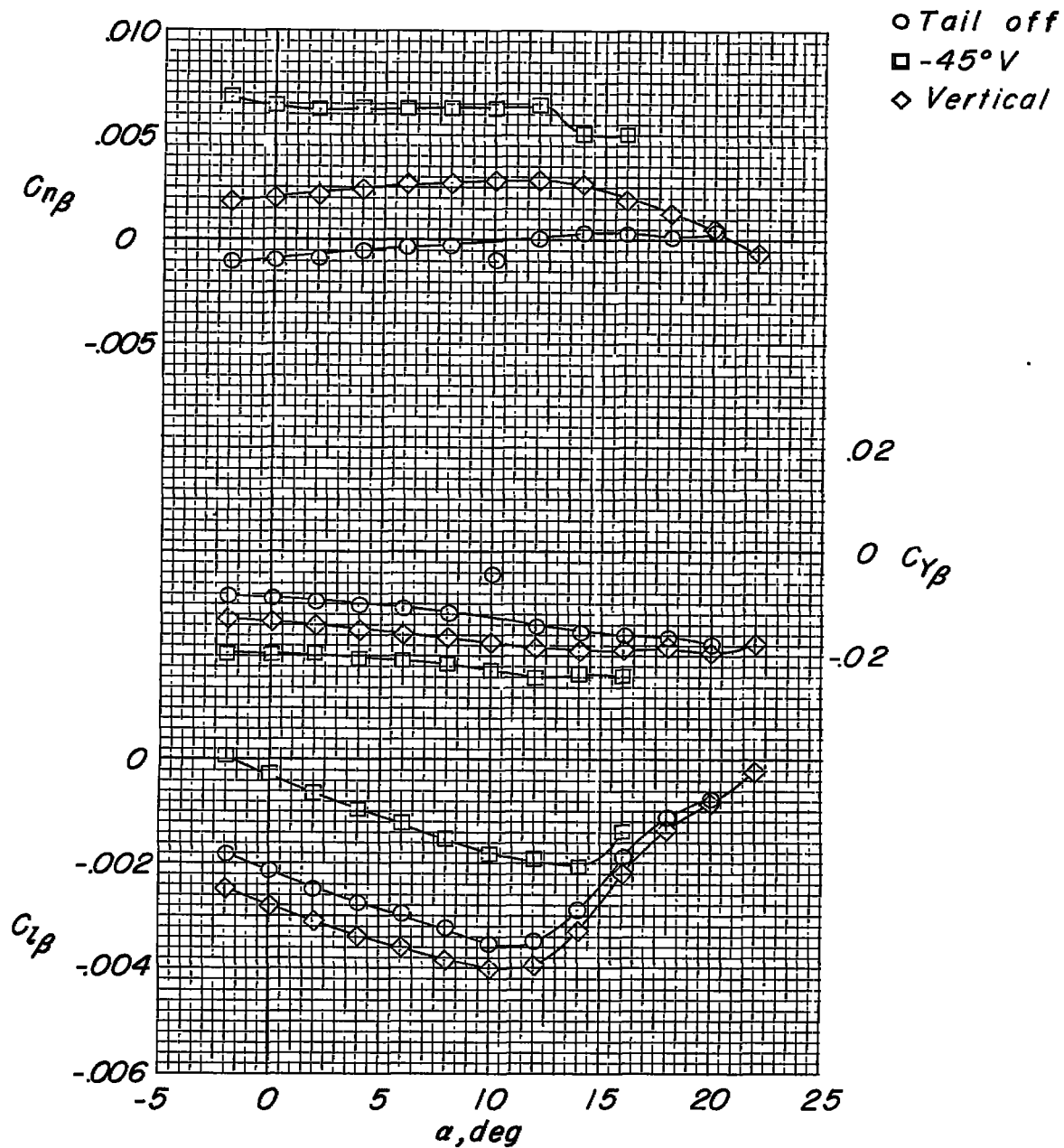
(c) $M = 0.85$.

Figure 8.- Continued.

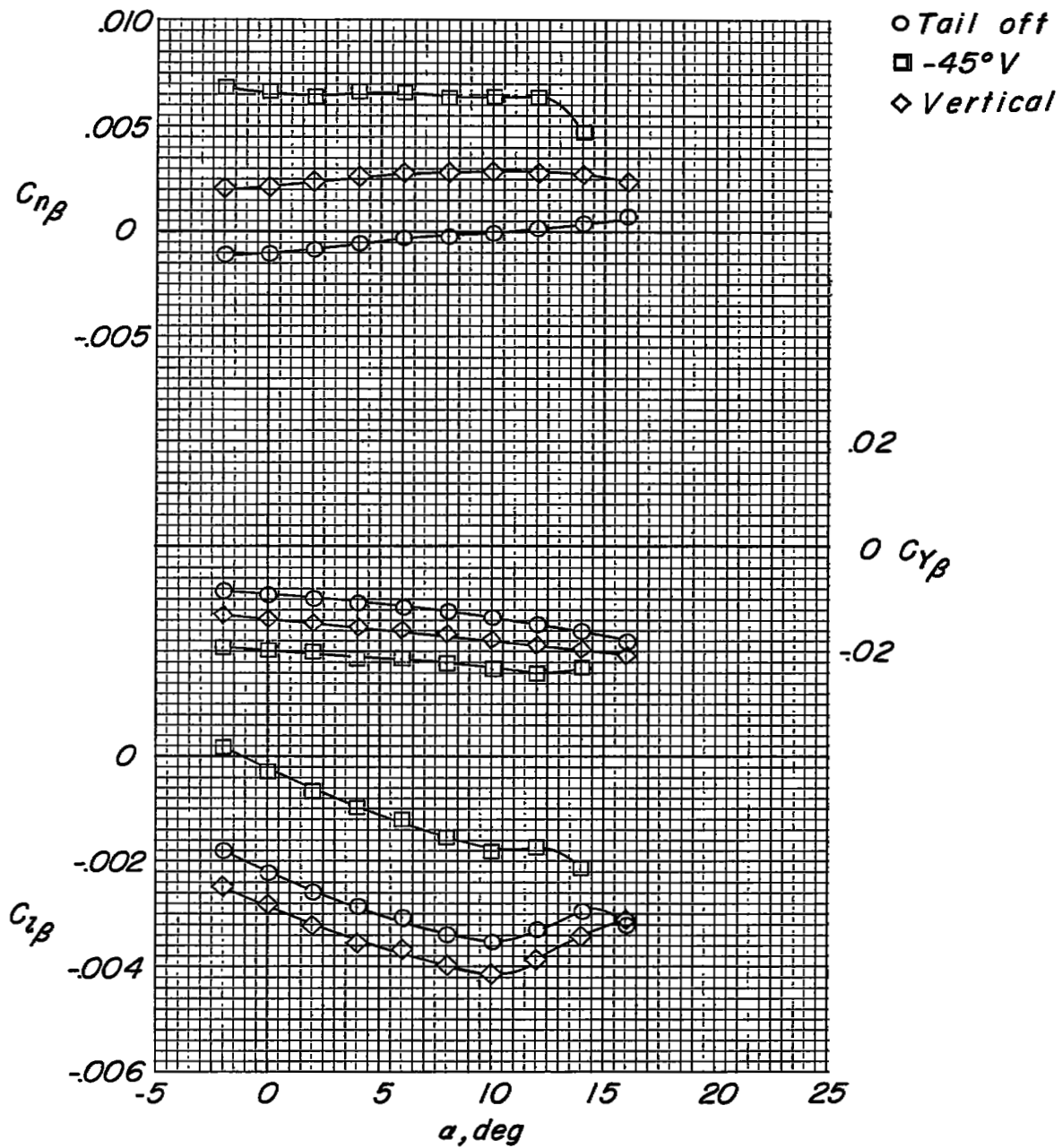
(d) $M = 0.90$.

Figure 8.- Continued.

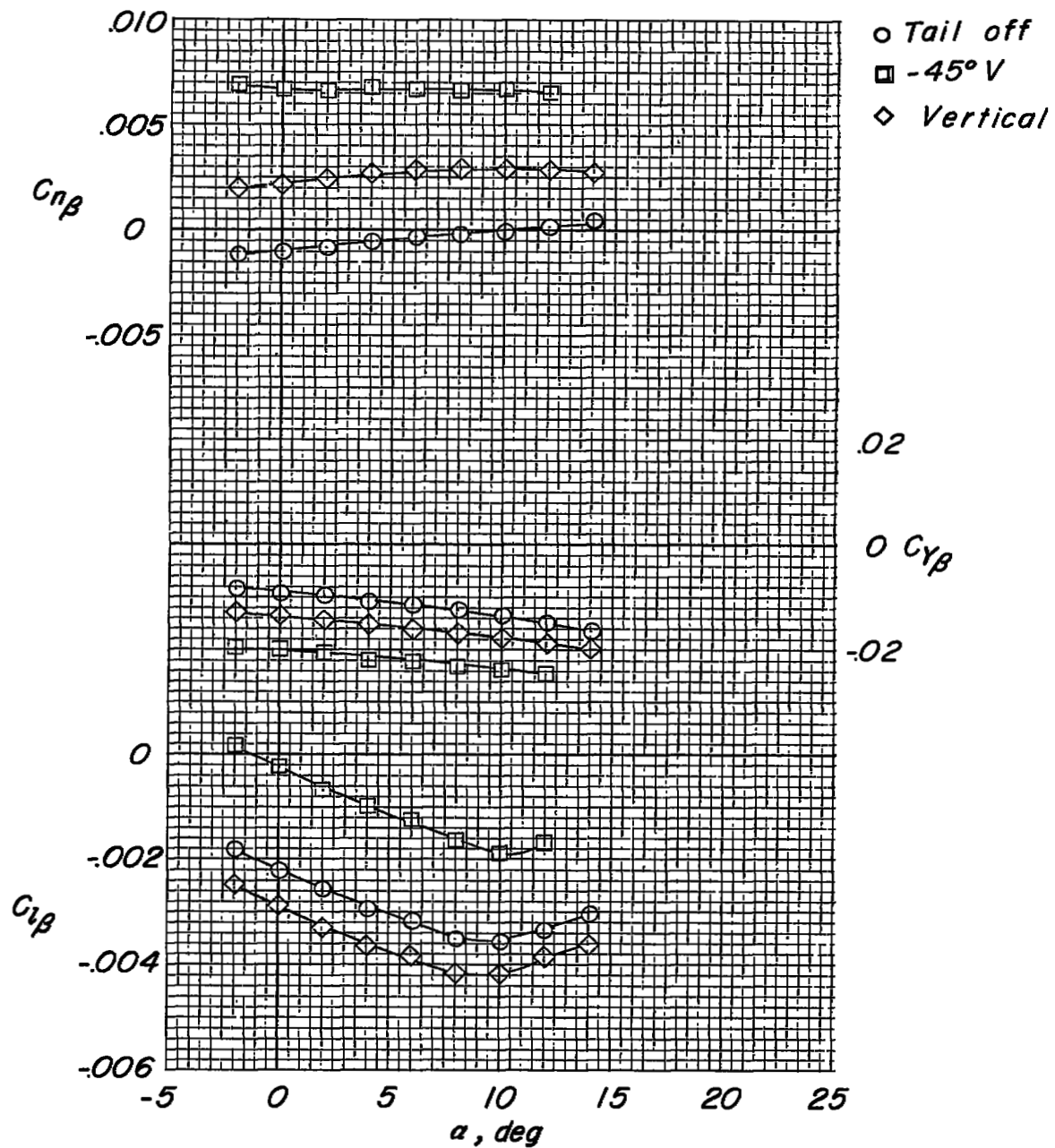
(e) $M = 0.92$.

Figure 8.- Concluded.

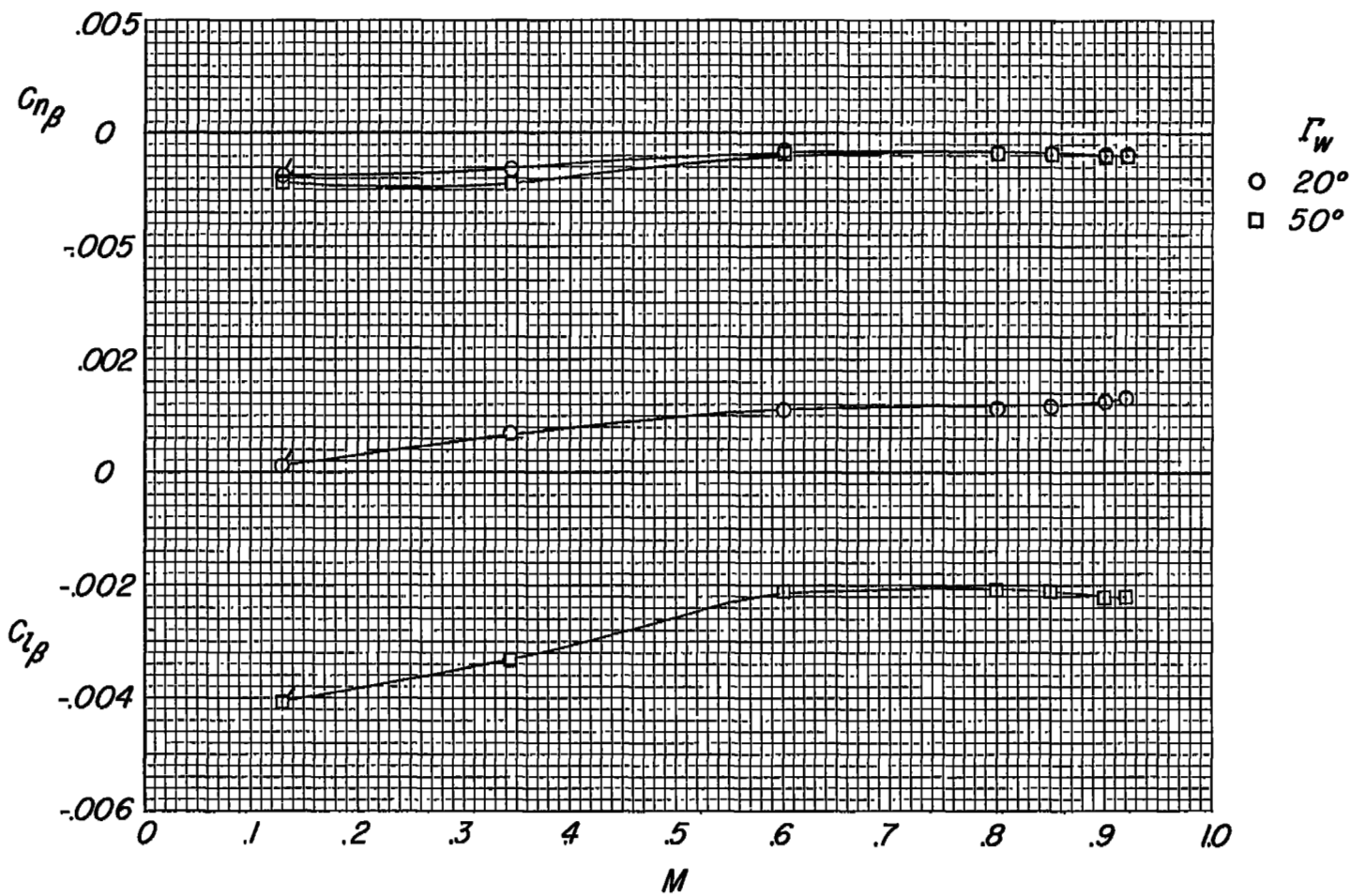


Figure 9.- Variation of $C_{n\beta}$ and $C_{l\beta}$ with Mach number for $\alpha = 0^\circ$.
 Flagged symbols are for data from reference 3.

CONFIDENTIAL